

Tuning in to Frequencies: How Global Assets Align U.S. Put–Call Parity Residuals

Useong Shin*

April 23, 2026

Abstract

Put–call parity holds under risk-neutral pricing, yet enforcement exposes arbitrageurs to path-dependent capital costs. The carry gap—the annualized wedge between option-implied and OIS discount factors—is a Q-measure object, but P-measure investment opportunities may shape its enforcement burden. We document this alignment in SPX and RUT options: low-frequency global asset returns raise in-sample R^2 by 0.093 and 0.082 and lift pooled out-of-sample R^2 from 0.221 to 0.364 (SPX) and 0.171 to 0.309 (RUT). Effective horizons differ by asset—IEFA (70 days), IGOV (400 days), IAU (336 days)—and asset terms largely absorb the OIS baseline, providing systematic evidence of a P→Q channel.

JEL: G12; G13; G14;

Keywords: carry gap; put–call parity; parity violation; path risk; limits to arbitrage; P–Q tension

*Sogang Business School, Sogang University (Seoul, Korea).
ORCID: [0009-0003-0197-9003](https://orcid.org/0009-0003-0197-9003)
Email: useong@sogang.ac.kr

1 Introduction

Put–call parity is the most basic no-arbitrage relation for European options. Viewed solely through its terminal payoff, it is a model-free identity, and under the risk-neutral measure its residual is zero by construction. Enforcing this identity in practice, however, requires holding a position exposed to path-dependent mark-to-market losses, margin requirements, and capital constraints. [Shin \(2026\)](#) documents that this enforcement burden manifests as a systematic wedge between option-implied and OIS discount factors—the *carry gap*—and characterizes it as a reduced-form function of a GBM path-risk term, trading frictions, and financial conditions.

Within the standard risk-neutral framework, the carry gap is a \mathbb{Q} -measure object constructed entirely from the discount structure inside the options market. Were this framework complete, \mathbb{P} -measure (physical) asset returns would have no structural reason to load on it: risk-neutral pricing is designed to operate with physical probabilities and expected returns explicitly neutralized. A systematic alignment between \mathbb{P} -measure asset returns and the carry gap would therefore constitute direct evidence that the risk-neutral framework is structurally silent on the economic burden of parity enforcement.

This paper documents such an alignment in the SPX and RUT options markets. Augmenting the baseline specification with low-frequency \mathbb{P} -measure return components from major global asset classes raises the explanatory power of the carry gap by $\Delta R^2 = 0.093$ in SPX and $\Delta R^2 = 0.082$ in RUT. The improvement is not confined to in-sample fit. Pooled out-of-sample R^2 rises from 0.221 to 0.364 in SPX and from 0.171 to 0.309 in RUT, with gains repeated across many holdout years in both markets. Notably, introducing the asset-return components produces an absorption pattern: much of the low-frequency variation previously captured by the OIS-based GBM terms is taken over by the \mathbb{P} -measure return components. This indicates that the structure picked up indirectly by the baseline through \mathbb{Q} -measure components is more directly tied to \mathbb{P} -measure investment opportunities, and can be read as systematic empirical evidence of a $\mathbb{P} \rightarrow \mathbb{Q}$ channel.

This economic logic is not naturally tied to put–call parity alone. More generally, any arbitrage that involves a futures or forward leg and is exposed to interim mark-to-market losses, variation margin, and finite-capital constraints may admit a similar implementation-risk term. A preliminary exploration of CIP deviation residuals across major currencies finds that a GBM term scaled by FX volatility delivers non-trivial explanatory power. These results are preliminary and lie outside the formal scope of this paper, but they suggest that the mechanism documented here is unlikely to be specific to equity index options and may extend to a broader parity-enforcement environment.

The paper makes four contributions. First, the residual of the most model-free no-arbitrage relation is not separable from P-measure investment opportunities, indicating that Q-measure pricing fails to internalize the P-measure costs of enforcement. Whereas the existing literature has focused on the Q→P direction—recovering P-measure expected returns from Q-measure objects—this paper provides evidence of the reverse P→Q channel, through which P-measure opportunities shape the enforcement burden of Q-measure pricing relations. Second, the asset classes with the strongest explanatory power are repeatedly concentrated in non-U.S. markets. An alternative specification built solely from U.S. equities and bonds is systematically weaker than the non-U.S. developed-market specification, both in- and out-of-sample, indicating that the outside-option channel for parity enforcement is linked to a global investment-opportunity set broader than U.S. domestic asset classes. Third, the effective horizon at which each asset class aligns with the carry gap differs sharply across assets (IEFA: 70 trading days; IGOV: 400; IAU: 336). This horizon heterogeneity suggests that the opportunity-cost structure of parity enforcement does not reduce to a single representative asset or common frequency, but is composed of multiple low-frequency components. Fourth, the economic content of the GBM term is best read not as a reduced-form artifact specific to a particular options-market regime, but as a broader reduced-form object summarizing the implementation burden of arbitrage strategies that involve a futures or forward leg; the preliminary CIP results offer an initial cue toward this interpretation.

The remainder of the paper proceeds as follows. Section 2 reviews the related literature. Section 3 lays out the analytical framework and baseline specification. Section 4 develops the asset-return extension and the derivation of the 3ETF specification. Section 5 reports the empirical results. Section 6 conducts robustness checks. Section 7 discusses the economic interpretation and implications, and Section 8 concludes.

2 Related Literature

This paper connects to several strands of literature on put–call parity. One concerns the theoretical formulation and empirical testing of the parity relation; another interprets observed deviations as the product of market frictions and limits to arbitrage. The paper also relates to the literature that estimates implied discount factors or funding conditions from option prices, and to the literature linking risk-neutral objects to physical-measure expected returns.

2.1 Put–Call Parity and Empirical Deviations

Put–call parity was systematically formalized by [Stoll \(1969\)](#), and the subsequent empirical literature has centered on whether observed deviations represent genuine arbitrage opportunities or reflect execution costs and constraints ([Gould and Galai, 1974](#); [Klemkosky and Resnick, 1979](#); [Ackert and Tian, 2001](#)). The shared conclusion is that observed deviations are better understood as empirical departures under execution frictions than as failures of no-arbitrage logic. This literature, however, has focused primarily on the existence of deviations and has paid less attention to how they are structured over time, and in particular to how they relate to asset returns outside the options market.

2.2 Limits to Arbitrage and Implementation Risk

This perspective has been developed more generally in the limits-to-arbitrage literature. Following [Shleifer and Vishny \(1997\)](#), subsequent work shows that arbitrage is exposed to funding constraints, margin requirements, path-dependent profits and losses, and finite-capital problems, so that theoretical price deviations need not be eliminated immediately ([Gromb and Vayanos, 2002](#); [Brunnermeier and Pedersen, 2009](#); [Mitchell and Pulvino, 2012](#)). In the options-market context, [Ofek et al. \(2004\)](#) show that short-sale constraints and limits to arbitrage can be linked to parity deviations. [Muravyev et al. \(2025\)](#) further demonstrate that much of the predictive power for individual stock returns attributed to implied-volatility spreads and skews in single-stock options reflects a measurement artifact arising from the omission of stock borrow fees in the implied-volatility calculation. The SPX and RUT contracts examined here are index options, for which borrow fees are effectively negligible; moreover, the carry gap is constructed from the wedge between option-implied and OIS discount factors rather than from implied-volatility spreads, distinguishing it from the borrow-fee channel identified by [Muravyev et al. \(2025\)](#).

I inherit the broader concerns of this literature but depart from it in two respects: I aggregate parity deviations into a daily time-series object and link them to asset-return-based state variables. Whereas the limits-to-arbitrage literature primarily addresses the persistence of deviations in price space, I show that a systematic wedge in carry space aligns with the physical-measure returns of the alternative investment opportunities the enforcer faces.

2.3 Conceptual Connection to CIP Deviations

[Du et al. \(2018\)](#) document that, since the global financial crisis, CIP deviations have been

persistently and systematically observed across G10 currencies, with magnitudes tied to quarter-end balance-sheet constraints, intermediary balance-sheet costs, and other fixed-income liquidity spreads. Their results indicate that deviations from textbook no-arbitrage relations may reflect not transitory frictions but a systematic price wedge embedding real-world intermediation costs and capital constraints.

I document the same phenomenon for put–call parity in equity index options, but with a different measurement object and a different explanatory channel. Whereas [Du et al. \(2018\)](#) examine the cross-currency basis in FX swap markets, I construct a carry gap from the wedge between option-implied and OIS discount factors and link it to low-frequency components of global asset returns.

2.4 Risk-Neutral Objects and Physical-Measure Expected Returns

The motivating question of this paper directly engages the literature on the relationship between risk-neutral objects extracted from option prices and physical-measure expected returns or risk premia. [Ross \(2015\)](#) provides conditions under which physical probabilities can be recovered from state prices; [Bollerslev et al. \(2009\)](#) show that the variance risk premium can be linked to expected stock returns; and [Martin \(2017\)](#) shows that the risk-neutral variance obtained from option prices can carry information about expected market returns. The common direction of this literature is the recovery of P-measure expected returns from Q-measure objects—that is, information extraction in the Q→P direction. I provide complementary evidence in the opposite direction. The result that physical-measure asset returns load systematically on the carry gap, itself a Q-measure object, points to the existence of a P→Q channel through which P-measure investment opportunities shape the enforcement burden of Q-measure pricing relations.

The structure I uncover—multiple asset classes loading on the carry gap at distinct horizons—is also conceptually consistent with the ICAPM of [Merton \(1973\)](#), in which investors hedging variation in the future investment-opportunity set are exposed to multiple state variables with heterogeneous time structures. A structural test of this connection lies beyond the scope of this paper and is left for future research.

2.5 Option-Implied Discount Factors and Closely Related Work

[Azzone and Baviera \(2021\)](#) estimate option-market-implied discount factors from European put–call parity and propose an empirical pipeline for comparing them against an exogenous discount benchmark. I adopt this approach directly to construct the carry gap and use it as the starting point of the analysis.

This paper also extends [Shin \(2026\)](#). [Shin \(2026\)](#) documents the existence and basic state-dependence of the carry gap and introduces a GBM path-risk kernel that summarizes the reduced-form structure of the enforcement burden. Building on that baseline specification, I explicitly introduce physical-measure asset-return components in order to identify the P-measure opportunity-cost channel on which the risk-neutral framework is structurally silent.

3 Framework and Baseline Specification

3.1 Identification of Option-Implied Discount Factors and the Carry Gap

I estimate option-market-implied discount factors following the identification procedure of [Azzone and Baviera \(2021\)](#). For European calls and puts at time t sharing maturity T and strike K , put–call parity can be written as

$$C_t(K, T) - P_t(K, T) = B_t(T)(F_t(T) - K), \quad (1)$$

where $B_t(T)$ is the market-implied discounting factor and $F_t(T)$ the forward value at the same maturity.

The key idea of [Azzone and Baviera \(2021\)](#) is to use the synthetic forward

$$\mathcal{G}_t(K, T) = C_t(K, T) - P_t(K, T) \quad (2)$$

to identify the discount factor $\hat{B}_t(T)$ that renders the recovered forward value flat across strikes. I apply this procedure repeatedly to the full SPX and RUT samples, producing a panel of option-implied discount factors indexed by market, date, and maturity.

The benchmark discount factor is taken from the OIS curve. The carry gap is defined as the annualized wedge between the option-implied and OIS discount factors. Letting $\tau_t(T) = T - t$,

$$CG_t(T) = \frac{1}{\tau_t(T)} \log \left(\frac{D_t^{\text{OIS}}(T)}{\hat{B}_t(T)} \right), \quad (3)$$

and in the empirical analysis I use the basis-points version

$$CG_t^{bp}(T) = 10^4 \cdot CG_t(T). \quad (4)$$

In the regression analysis, the daily-aggregated market-level carry gap is denoted $CG_{i,t}^{bp}$.

3.2 Construction of the GBM Term

I introduce the GBM term as a reduced-form component summarizing the path-dependent risk and capital commitment of parity enforcement. Although a parity position is deterministic at the terminal payoff, maintaining it before maturity is not frictionless: the trader remains exposed to interim mark-to-market losses, margin requirements, and the possibility of additional capital injections. The economic burden of enforcement may therefore vary systematically with volatility, time to maturity, and the opportunity cost of capital.

A simple way to formalize this intuition is to approximate the normalized interim profit-and-loss process by

$$X_t = \sigma B_t,$$

where B_t is a standard Brownian motion and σ denotes annualized volatility. Let L_t denote the minimum cumulative capital support needed to keep the position solvent throughout $[0, T]$. Under the minimal support rule,

$$L_t = \sup_{0 \leq s \leq t} (-X_s)^+.$$

A standard property of Brownian motion implies that the expected support at horizon t scales as

$$\mathbb{E}[L_t/N] = \sigma \sqrt{\frac{2t}{\pi}},$$

so the required support is proportional to volatility and rises with the square root of time. Averaging over the life of the trade gives the representative capital commitment

$$\bar{B}(T) = \frac{1}{T} \int_0^T \mathbb{E}[L_t/N] dt = \frac{2}{3} \sigma \sqrt{\frac{2T}{\pi}}.$$

If the opportunity cost of tied-up capital is summarized by a rate-like object r_t , the implied scaling is $r_t \bar{B}(T)$. The GBM term used in the empirical specification is simply this structure translated into basis points.

Accordingly, for market $i \in \{\text{SPX}, \text{RUT}\}$, I define

$$GBM_{i,t}^{\text{OIS},xY} = 10^4 \cdot \frac{\text{OIS}_t^{xY}}{100} \cdot \frac{2}{3} \cdot \frac{\text{Vol}_{i,t}}{100} \cdot \sqrt{\frac{2\tau_{i,t}}{\pi}}, \quad x \in \{1, 10\}, \quad (5)$$

where

$$\text{Vol}_{i,t} = \begin{cases} \text{VIX}_t, & i = \text{SPX}, \\ \text{RVX}_t, & i = \text{RUT}. \end{cases}$$

$GBM_{i,t}^{\text{OIS},1Y}$ and $GBM_{i,t}^{\text{OIS},10Y}$ can be read as baseline components reflecting the opportunity cost of capital at shorter and longer horizons, respectively. The purpose here is not to estimate a structural model of parity enforcement, but to embed in the empirical specification the core functional form suggested by path-dependent implementation risk.

3.3 Baseline Regression

The baseline specification is a separate regression that directly allows for cross-market heterogeneity. For each market $i \in \{\text{SPX}, \text{RUT}\}$,

$$CG_{i,t}^{bp} = \alpha_i + \phi_{1,i}GBM_{i,t}^{\text{OIS},1Y} + \phi_{10,i}GBM_{i,t}^{\text{OIS},10Y} + \beta_i \frac{BA_{i,t}^{med}}{\tau_{i,t}} + \gamma_i NFCI_t + \varepsilon_{i,t}, \quad (6)$$

where $BA_{i,t}^{med}$ is the median ATM bid–ask spread and $NFCI_t$ is the Chicago Fed National Financial Conditions Index.

This baseline, established in [Shin \(2026\)](#), is the starting point for the systematic link between the carry gap, the GBM term, trading frictions, and financial conditions. [Table 3.1](#) and [Table 3.2](#) report its in-sample and LOYO out-of-sample performance, respectively.

Table 3.1: In-sample fit of the baseline regression

Specification	Observations	Dates	R^2	Adj. R^2	RMSE (bp)	MAE (bp)
SPX	29,368	2,456	0.312	0.312	13.20	8.68
RUT	18,645	2,455	0.281	0.281	13.95	10.10

Table 3.2: LOYO out-of-sample performance of the baseline regression

Market	Mean R^2	Median R^2	Pooled R^2	Years with $R^2 > 0$	Mean correlation	Mean RMSE (bp)
SPX	0.059	0.130	0.221	7/10	0.205	13.95
RUT	0.075	0.108	0.171	6/10	0.243	15.07

The baseline explains roughly 28–31% of the in-sample variation in the carry gap and retains positive pooled R^2 out of sample under the LOYO scheme. The next section examines how much this explanatory power improves once asset-return components are added to the baseline.

4 Asset-Return Extension and Derivation of the 3ETF Specification

4.1 Motivation for Asset-Return Components

The central question raised in the introduction is whether physical-measure asset returns—explicitly neutralized by the risk-neutral framework—nonetheless load systematically on the carry gap, a Q-measure object. To test this empirically, I consider an extended specification that replaces the rate-like component of the baseline GBM term with low-frequency P-measure returns from major asset classes.

The baseline GBM term summarizes the path-dependent risk and capital commitment of parity enforcement as a combination of volatility, time to maturity, and a rate-like object. There is no a priori reason to restrict that rate-like object to the OIS rate. Real-world arbitrageurs are not mechanical parity enforcers but economic agents allocating capital across competing asset classes, so the opportunity cost of parity enforcement may be tied not only to a particular interest rate level but also to low-frequency returns on alternative investments. The empirical question is then narrow and concrete: which asset, at which horizon, aligns most closely with the carry gap in U.S. index options markets? I address this question with an asset-by-asset horizon scan over alternative lookback windows.

To suppress high-frequency noise, I use the OLS slope of log prices over a lookback window of n trading days rather than a simple cumulative return. To preclude look-ahead bias, the slope used at date t is computed from information through $t - 1$ only and excludes the contemporaneous price. Formally, the low-frequency return component for asset a , $\tilde{r}_{a,t}^{(n)}$, is the slope of a linear approximation to the most recent n -day log-price path ending at $t - 1$. This construction reflects persistent trend components more stably than transient spikes.

4.2 Single-Asset Explanatory Power and Horizon Profiles

I begin by examining how the incremental R^2 over the baseline separate regression varies across lookback horizons for each candidate asset. The candidate set comprises ten low-cost ETFs representing the major asset classes.¹ For each ETF, the log OLS slope at lookback n serves as the asset-return-based low-frequency component.

¹VTI (U.S. equity), IEFA (developed ex-U.S. equity), IEMG (emerging-market equity), BND (U.S. aggregate bond), SCHP (U.S. inflation-linked bond), IGOV (developed ex-U.S. sovereign bond, FX-unhedged), EBND (emerging-market sovereign bond, FX-unhedged), IAU (gold), VNQ (U.S. REITs), VNQI (ex-U.S. REITs).

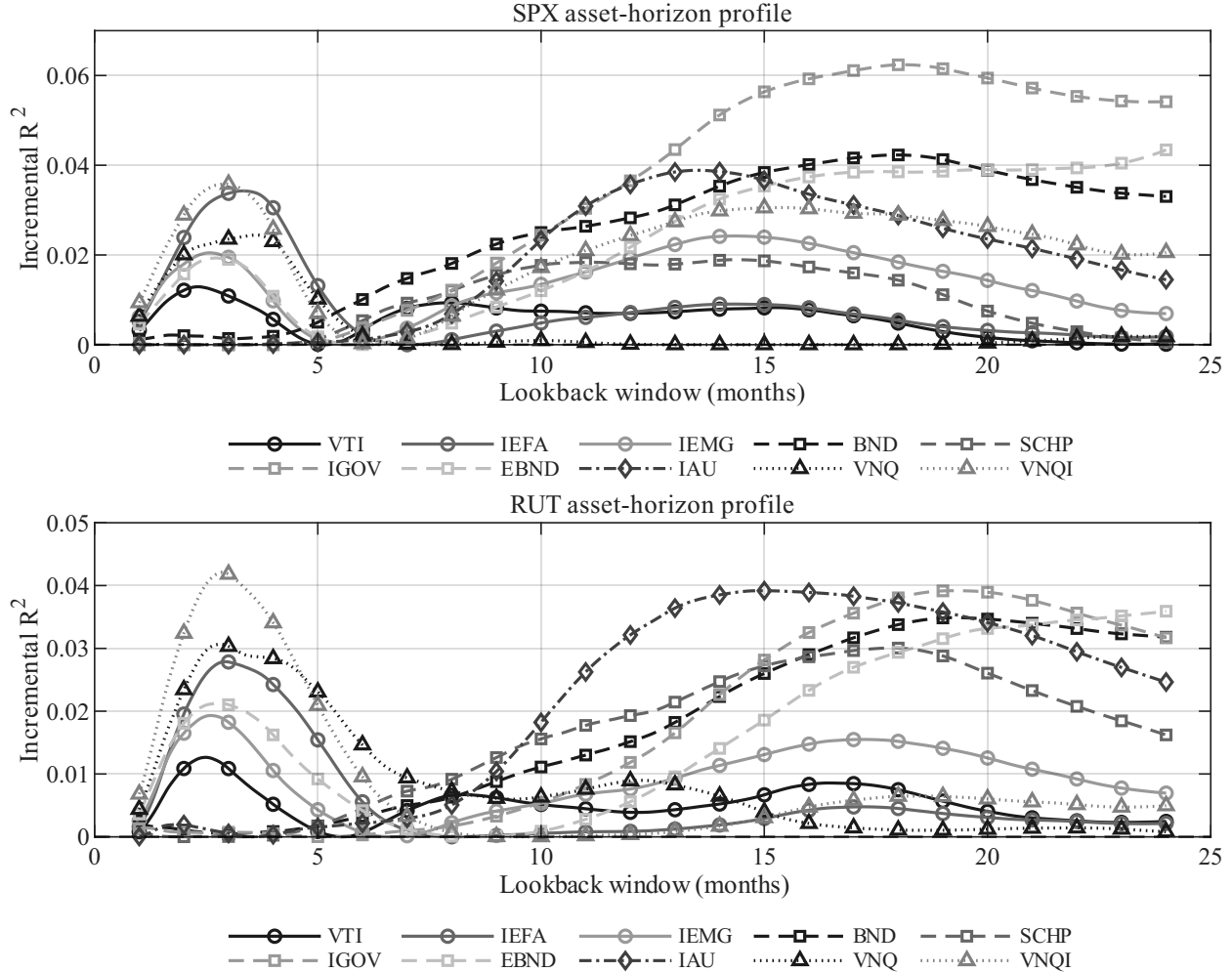


Figure 4.1: Incremental R^2 by lookback horizon for ETFs representing the major asset classes. The effective lookback horizon at which each asset aligns with the carry gap differs sharply across assets. The upper panel shows SPX results; the lower panel, RUT.

The key feature of Figure 4.1 is not the magnitude of the explanatory gains but the location of the horizon at which they appear. IEFA, the developed ex-U.S. equity proxy, gains explanatory power quickly at relatively short horizons and peaks early. IGOV, the international government bond proxy, improves at much longer horizons and peaks deep in the long-end region. IAU, the gold proxy, shows stable gains over a medium-to-long horizon range that lies between those of IEFA and IGOV. The “frequency” at which low-frequency components align with the carry gap thus differs across asset classes.

These profiles also indicate that the gains are not knife-edge artifacts of a single window. For the assets retained in the main specification, the high- R^2 region around each peak forms a relatively gentle plateau, so the final window choices are best understood as compromises representing each asset’s effective horizon band rather than pointwise optima.

4.3 Selection of the 3ETF Specification under a Minimalist View

Among the candidate assets, the main specification restricts attention to three ETF components, balancing explanatory power against parsimony. Following the conventional asset-allocation taxonomy, I select one equity, one bond, and one gold proxy, and consider three combinations along a regional axis: a U.S.-centered combination (VTI, BND, IAU), a developed ex-U.S. combination (IEFA, IGOV, IAU), and an emerging-market-centered combination (IEMG, EBND, IAU). The developed ex-U.S. combination delivers the strongest in-sample explanatory power overall and is therefore adopted as the main specification; the other two are revisited as alternative-asset robustness checks in Section 6.2.

The selected assets are thus IEFA (developed ex-U.S. equity), IGOV (international government bond), and IAU (gold). They represent distinct economic categories, reducing explanatory overlap while spanning a broad outside-option set. All three deliver meaningful incremental R^2 over the baseline in single-asset scans, repeatedly in both markets, and among the strongest candidates the non-U.S. assets tend to deliver larger incremental R^2 than their U.S. counterparts. This pattern suggests that the outside-option channel aligned with the carry gap is connected to a global investment- opportunity set broader than U.S. domestic asset classes. The main specification is therefore not the result of mechanically adding many assets, but of combining a minimal set of strong-explanatory non-U.S. candidates with heterogeneous frequencies.

The final lookback windows are 70 trading days for IEFA, 400 for IGOV, and 336 for IAU. The high-explanatory-power regions form relatively gentle plateaus over 70–84 days for IEFA, 294–400 days for IGOV, and 315–357 days for IAU. The pointwise optima differ slightly between SPX and RUT, but each chosen window lies within the respective plateau in both markets. The values therefore preserve a single specification applicable to both markets while still representing each asset’s high-explanatory band.

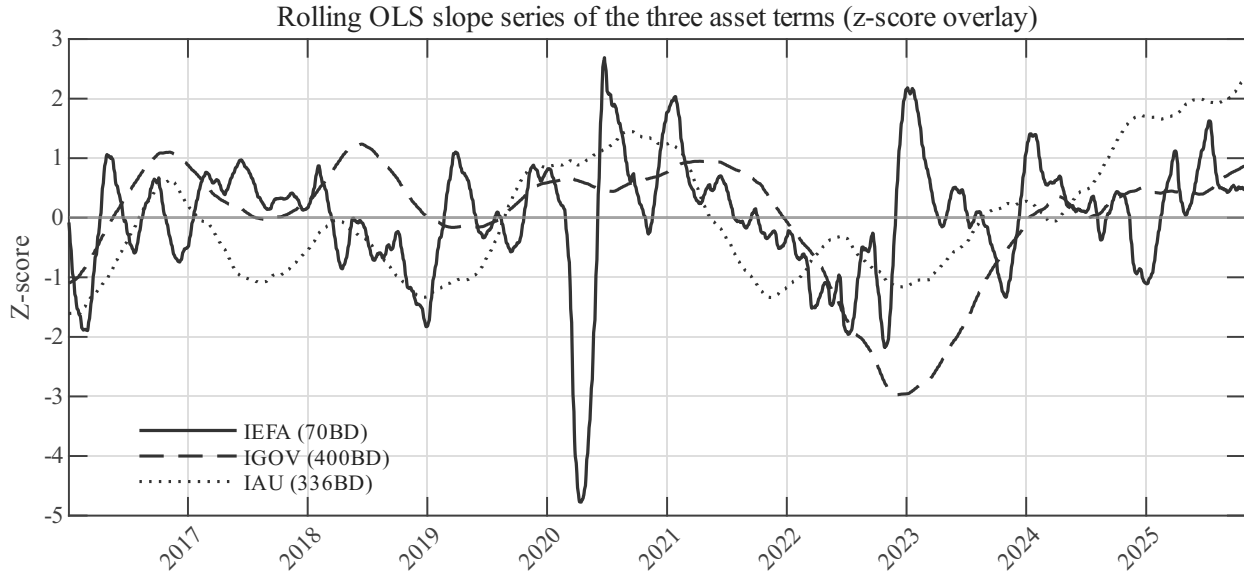


Figure 4.2: OLS slope time series for the three selected ETFs. Each series is the log OLS slope under the lookback window adopted in the main specification (IEFA: 70 days; IGOV: 400; IAU: 336), standardized as a z -score.

Figure 4.2 compares the standardized OLS-slope series of the three selected ETFs. Although each is the same type of asset-return component, the choice of lookback window induces low-frequency dynamics of distinctly different speeds. The IEFA component moves comparatively quickly, the IGOV component varies far more slowly and smoothly, and the IAU component sits in between. The horizon heterogeneity identified in the scan therefore reflects not a coincidence at the R^2 level but a real difference in time-series dynamics. The 3ETF specification is thus best read as a minimalist combination of assets representing distinct low-frequency components, rather than as an arbitrary parallel addition of high- R^2 regressors.

Figure 4.2 also serves as an indirect falsification test against the hypothesis that the explanatory power of the 3ETF specification merely repackages a single common factor—the global financial cycle or a broad-dollar factor, for instance. Under such a single-factor null, the rolling slopes of the three assets should share a common low-frequency trajectory. IGOV (400 days) and IAU (336) display roughly similar low-frequency envelopes, consistent with partial exposure to a common component—an exposure directly confirmed for IGOV by the FX-neutralization results of Section 6.1. IEFA (70 days), however, retains substantial higher-frequency variation that the slow envelope cannot absorb: a deep dip to roughly -4.7 in early 2020, positive excursions in mid-2020 and early 2021, and a sharp sign reversal during the 2022–2023 transition all show episode-specific behavior that departs visibly from the slower trajectories of IGOV and IAU. The three slope series therefore do not collapse to a

single latent factor: at minimum, an IEFA-specific high-frequency channel coexists with the slower dynamics of IGOV and IAU, supporting a multi-channel structure. The improvement delivered by the 3ETF specification is thus unlikely to be a mere indirect restatement of a single global factor, and the cross-asset frequency heterogeneity documented earlier is visible not only at the R^2 level but also in the slope dynamics themselves.

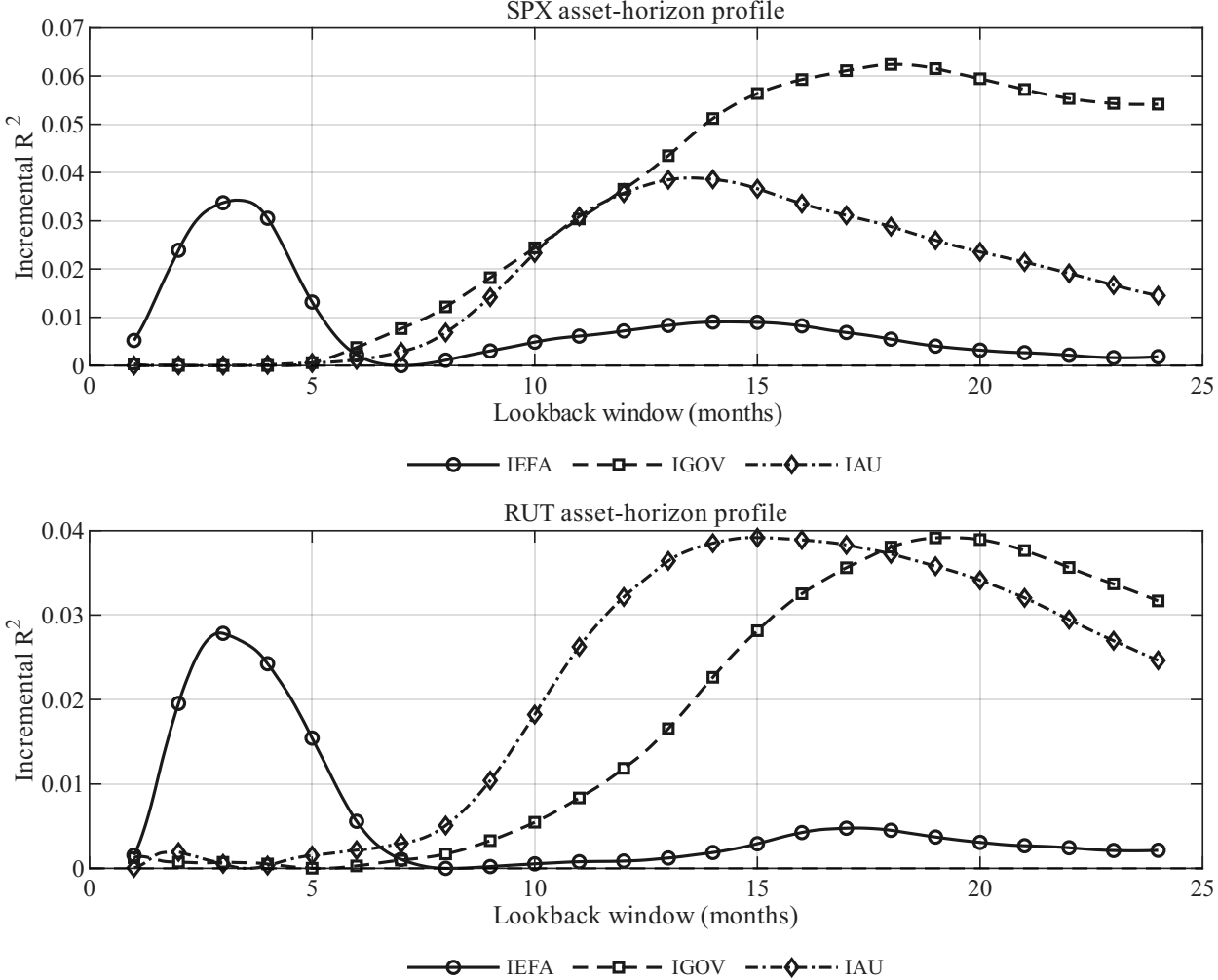


Figure 4.3: Incremental R^2 by lookback horizon for the three selected ETFs. The upper panel shows SPX results; the lower panel, RUT.

Figure 4.3 zooms in on the per-market horizon scan for the three selected ETFs. IEFA shows comparatively large incremental R^2 at short horizons, IGOV at long horizons, and IAU at medium-to-long horizons. The pattern is broadly common to both SPX and RUT.

4.4 The Final 3ETF Regression

Building on these results, the final extended specification augments the baseline separate regression with three asset-return-based GBM terms. For asset a and lookback n , the asset-return-based GBM term is constructed by replacing the rate-like object in the baseline GBM term with $\tilde{r}_{a,t}^{(n)}$. The final regression for market $i \in \{\text{SPX}, \text{RUT}\}$ is then

$$\begin{aligned}
 CG_{i,t}^{bp} = & \alpha_i + \phi_{1,i}GBM_{i,t}^{\text{OIS},1Y} + \phi_{10,i}GBM_{i,t}^{\text{OIS},10Y} \\
 & + \theta_{E,i}GBM_{i,t}^{\text{IEFA},70} + \theta_{G,i}GBM_{i,t}^{\text{IGOV},400} + \theta_{A,i}GBM_{i,t}^{\text{IAU},336} \\
 & + \beta_i \frac{BA_{i,t}^{med}}{\tau_{i,t}} + \gamma_i NFCI_t + \varepsilon_{i,t}.
 \end{aligned} \tag{7}$$

Here $GBM_{i,t}^{\text{IEFA},70}$, $GBM_{i,t}^{\text{IGOV},400}$, and $GBM_{i,t}^{\text{IAU},336}$ are the asset-return-based GBM terms constructed by using the 70-day, 400-day, and 336-day log OLS slopes of IEFA, IGOV, and IAU, respectively, as the rate-like component. The final specification thus layers an additional low-frequency outside-option component—supplied by foreign equity, foreign sovereign bond, and gold—on top of the generic capital-opportunity-cost component captured by the baseline OIS-based GBM term.

The next sections examine, in order, the in-sample fit, out-of-sample performance, and time-series fit of equation (7).

5 Empirical Results

This section compares the empirical performance of the 3ETF extended specification against the baseline separate specification. I begin with a visual comparison of fit on the maturity-pooled daily series, then turn to in-sample fit, the coefficient structure, and out-of-sample performance. Coefficient interpretation and statistical inference are based on date-based HAC (Newey–West) standard errors.

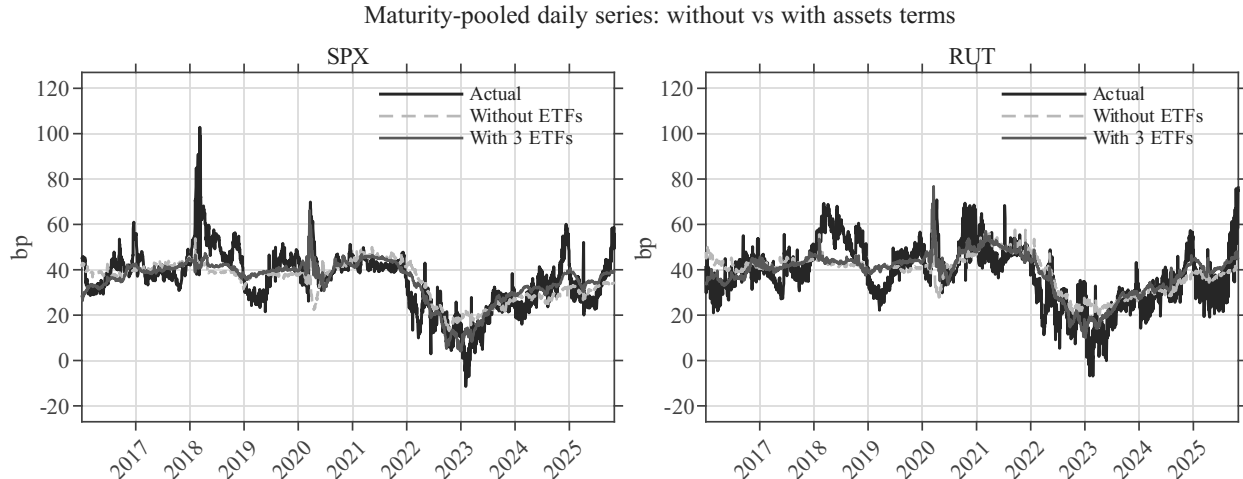


Figure 5.1: Maturity-pooled daily fit: baseline separate specification versus 3ETF extended specification. The left panel shows SPX; the right panel, RUT. In both markets the 3ETF specification tracks the low-frequency variation in the actual carry gap more closely than the baseline.

Figure 5.1 compares the fitted values of the baseline and the 3ETF specification on the maturity-pooled daily series for both markets. In both SPX and RUT, the 3ETF specification follows the direction and level variation of the actual carry gap more closely than the baseline, and in particular captures the low-frequency movements around regime transitions that the baseline misses.

5.1 In-Sample Performance

Table 5.1: In-sample performance: baseline versus 3ETF extended specification

Market	R^2 (baseline)	R^2 (3ETF)	ΔR^2	ΔRMSE (bp)	ΔMAE (bp)
SPX	0.312	0.405	0.093	-0.924	-0.976
RUT	0.281	0.363	0.082	-0.816	-0.695

Table 5.1 shows that the extended specification delivers a clear in-sample improvement in both markets, with $\Delta R^2 = 0.093$ in SPX and $\Delta R^2 = 0.082$ in RUT, and lower RMSE and MAE in both. The fit statistics themselves are essentially unchanged whether or not HAC inference is applied, so the explanatory gain of the 3ETF specification does not depend on the choice of standard-error estimator.

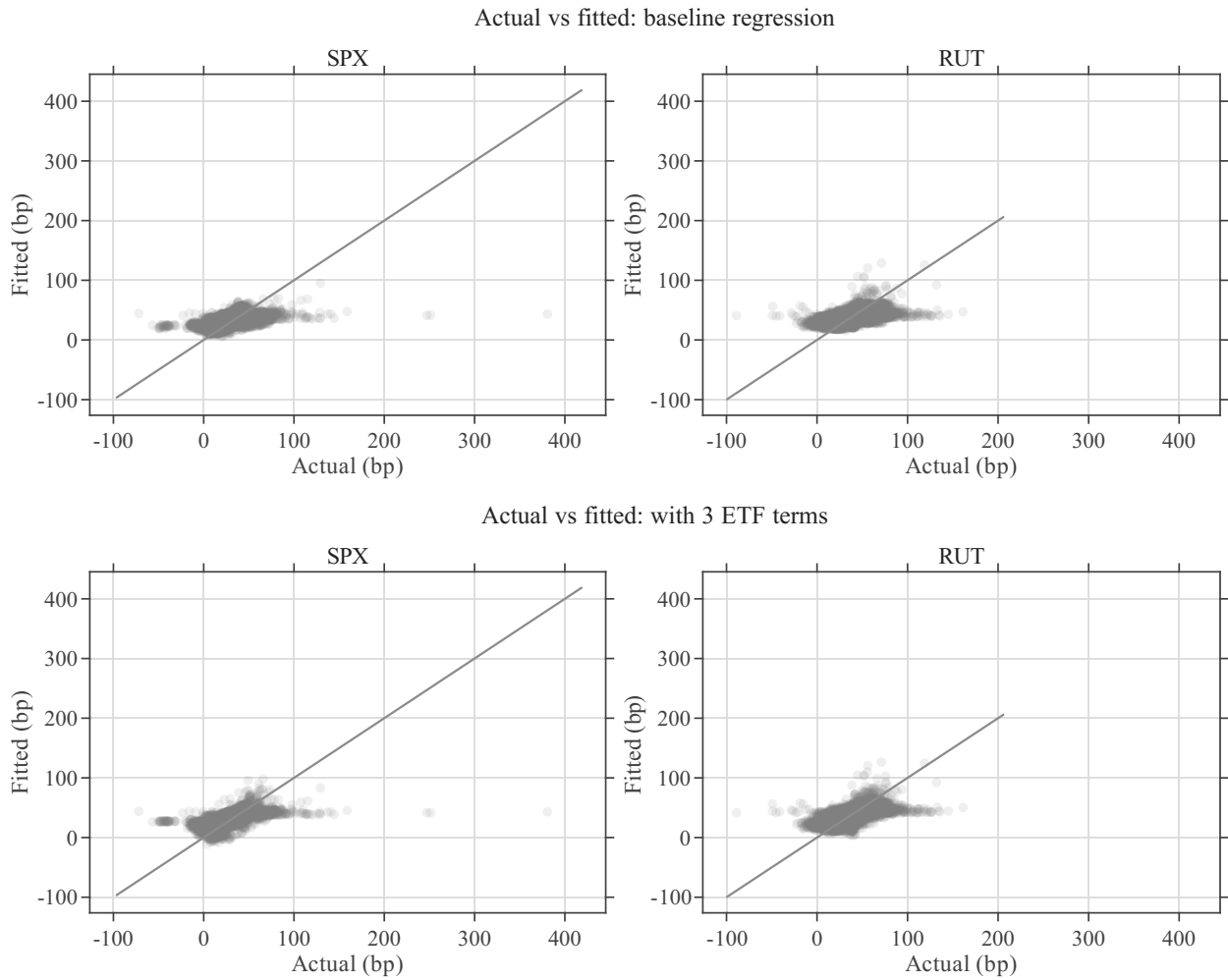


Figure 5.2: Fitted versus actual scatter plots: baseline versus 3ETF extended specification. The upper panel shows the baseline separate regression; the lower panel, the 3ETF extended regression. Under the 3ETF specification, observations cluster more tightly along the 45° line, providing a visual confirmation of the in-sample improvement.

Figure 5.2 shows that this improvement is not limited to summary statistics. Once the 3ETF components are added, observations cluster more tightly around the 45° line, and the variation that the baseline systematically undershot is reflected more faithfully.

5.2 Coefficient Structure

Table 5.2: In-sample regression coefficients: baseline versus 3ETF extended specification, HAC inference

Regressor	SPX baseline	SPX + 3ETF	RUT baseline	RUT + 3ETF
Intercept	23.134*** (5.713)	19.603*** (4.298)	24.577*** (5.407)	14.773*** (3.670)
$GBM^{OIS,1Y}$	-0.548*** (0.170)	-0.029 (0.118)	-0.555*** (0.124)	-0.181** (0.075)
$GBM^{OIS,10Y}$	0.411** (0.172)	-0.111 (0.134)	0.541*** (0.130)	0.102 (0.091)
$GBM^{IEFA,70}$	—	-0.00887*** (0.00155)	—	-0.00712*** (0.00114)
$GBM^{IGOV,400}$	—	0.0433*** (0.0149)	—	0.00907 (0.0118)
$GBM^{IAU,336}$	—	0.0121 (0.00737)	—	0.0221*** (0.00509)
BA^{med}/τ	0.256*** (0.0635)	0.203*** (0.0665)	0.130*** (0.0225)	0.130*** (0.0256)
$NFCI$	-25.839** (10.359)	-35.652*** (7.827)	-23.961** (10.013)	-45.419*** (6.812)
R^2	0.3124	0.4053	0.2809	0.3626
Adj. R^2	0.3123	0.4051	0.2807	0.3623
RMSE (bp)	13.199	12.275	13.951	13.135
MAE (bp)	8.682	7.706	10.103	9.408

Notes: Standard errors in parentheses are date-based HAC (Newey–West, lag = 21). ***, **, and * denote statistical significance at the 1%, 5%, and 10% levels, respectively.

Table 5.2 reports the in-sample regression coefficients with date-based HAC (Newey–West, lag = 21) inference. The fit statistics remain high, but standard errors that account for serial dependence make it clearer which components remain statistically robust.

The most prominent common result is that the IEFA term carries a consistently negative sign and strong statistical significance in both markets. Foreign equity is therefore the asset-return-based channel that aligns most stably with the carry gap. The IGOV term loads with a significant positive coefficient in SPX but, while the sign is preserved in RUT, is statistically insignificant there. Symmetrically, the IAU term carries a strong positive coefficient in RUT but, while the SPX point estimate is positive and similar in magnitude, fails to reach conventional significance under lag 21 HAC. The asset-return component that

is robust across both markets is thus IEFA, with IGOV operating more visibly in SPX and IAU more visibly in RUT.

The sign structure is consistent with the paper’s interpretation of the carry gap as an implementation-risk premium. A positive carry gap in put–call parity means that the option-implied forward is priced rich relative to the OIS benchmark; this premium is paid by the arbitrageur enforcing parity through a forward-sale leg—the agent bearing path-dependent mark-to-market losses and capital commitment—to the forward buyer. Under this interpretation, the negative IEFA coefficient is consistent with periods in which strong low-frequency global risk-asset returns expand the enforcer’s risk-bearing capacity, compressing the premium required for a given path risk. The positive IAU and—more strongly in SPX—IGOV coefficients are consistent with the opposite case: in risk-off episodes that strengthen safe-asset demand, the enforcer’s capacity contracts and the premium widens. The three signs capture different phases by asset class but admit a single mechanism: variation in the enforcer’s risk-bearing capacity is reflected in the implementation- risk premium. This interpretation is based on the reduced-form alignment structure; structural identification of the mechanism is left for future research.

The HAC inference also reveals how much of the role of the OIS-based GBM terms is taken over once the 3ETF components are added. In SPX, neither $GBM^{OIS,1Y}$ nor $GBM^{OIS,10Y}$ remains statistically significant, indicating that much of the low-frequency variation captured by the OIS terms in the baseline is absorbed by the IEFA, IGOV, and IAU components. In RUT, $GBM^{OIS,1Y}$ remains significant at the 5% level, showing that the short-horizon OIS-based opportunity-cost channel is not fully displaced even after the asset-return components are introduced. Even in RUT, however, $GBM^{OIS,10Y}$ shrinks sharply from 0.541 in the baseline to 0.102 and turns insignificant.

The trading-friction and financial-conditions variables continue to play important roles. BA^{med}/τ remains positive and statistically significant in both markets and both specifications, indicating that the trading-friction channel operates on the carry gap independently of the asset-return components. $NFCI$ is significant only at the 5% level in the baseline but, under the 3ETF specification, takes on a larger negative coefficient with strong significance in both markets, showing that broad financial conditions continue to explain residual variation in the carry gap even after controlling for the asset-return-based low-frequency components.

The overall message survives lag 21 HAC inference: the dynamics of the carry gap, a Q-measure object, are not adequately summarized by OIS-based rate components inside the risk-neutral framework alone, and low-frequency asset-return components reflecting P-measure investment opportunities provide significant additional explanatory power. Among these components, however, the most robust common channel is IEFA, while IGOV and IAU

are best read at this stage as selective channels that operate with cross-market heterogeneity.

5.2.1 In-Sample Performance by Maturity Bin

Table 5.3: In-sample performance by τ bin: baseline versus 3ETF extended specification

Market	Maturity bin	R^2 (baseline)	R^2 (3ETF)	ΔR^2	$\Delta RMSE$ (bp)	ΔMAE (bp)
SPX	1–2m	0.096	0.145	0.049	-0.619	-0.649
SPX	2–3m	0.184	0.266	0.082	-0.920	-0.754
SPX	3–5m	0.283	0.414	0.130	-1.298	-0.949
SPX	5–7m	0.373	0.546	0.173	-1.710	-1.094
SPX	7–10m	0.472	0.643	0.171	-1.739	-1.144
SPX	10–14m	0.525	0.623	0.098	-0.903	-0.922
SPX	14–21m	0.306	0.332	0.026	-0.249	-1.084
SPX	21m+	0.182	0.139	-0.042	0.347	-1.034
RUT	1–2m	0.112	0.159	0.047	-0.596	-0.499
RUT	2–3m	0.205	0.300	0.095	-0.969	-0.611
RUT	3–5m	0.254	0.366	0.112	-1.011	-0.748
RUT	5–7m	0.231	0.422	0.191	-1.672	-1.255
RUT	7–10m	0.284	0.462	0.178	-1.578	-1.090
RUT	10–14m	0.472	0.559	0.086	-0.901	-0.894
RUT	14–21m	0.482	0.530	0.049	-0.487	-0.475
RUT	21m+	0.413	0.288	-0.125	1.083	0.564

Table 5.3 shows that the explanatory gains of the 3ETF specification are not uniformly distributed across maturity bins. In both markets, the gains are concentrated in the medium-maturity range, peaking around 5–10 months. In SPX, ΔR^2 reaches 0.173 at 5–7 months and 0.171 at 7–10 months, with R^2 levels of 0.546 and 0.643. The same bins yield the largest gains in RUT, with ΔR^2 of 0.191 and 0.178. Reaching R^2 values of 0.5–0.6 at the medium-maturity bins in a daily regression is notable.

At the very long end the pattern reverses: in the 21-month-plus bin, ΔR^2 is -0.042 in SPX and -0.125 in RUT. The parsimonious 3ETF specification therefore captures the dominant structure of the medium-maturity range effectively but appears to miss additional slow-moving low-frequency components or maturity-specific factors operating at the very long end.

5.3 Out-of-Sample Performance

I now assess the generalizability of the extended specification using leave-one-year-out (LOYO) validation. The central interest is whether the addition of the 3ETF components produces consistent performance gains across alternative holdout years rather than a one-off in-sample fit.

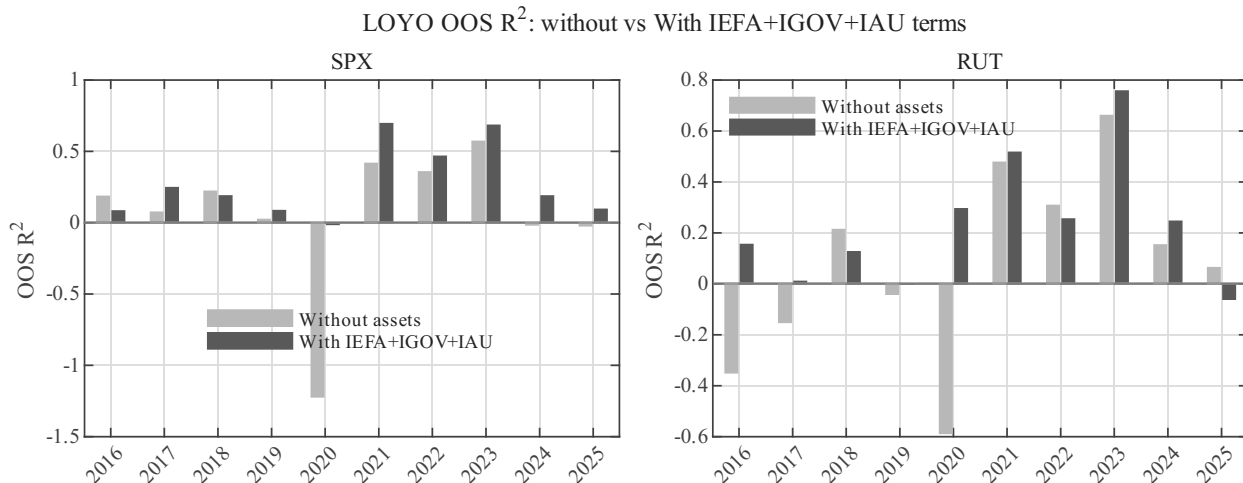


Figure 5.3: Year-by-year LOYO out-of-sample R^2 : baseline separate specification versus 3ETF extended specification. Bars in each panel show the holdout-year out-of-sample R^2 . The 3ETF specification delivers higher R^2 than the baseline in many holdout years in both markets, with especially clear improvements in years where the baseline performs poorly.

Figure 5.3 shows first that the improvement from the 3ETF specification is not confined to a few specific years. The 3ETF specification produces higher out-of-sample R^2 than the baseline in 8 of 10 holdout years for SPX and in 7 of 10 for RUT. The gains are most pronounced in years where the baseline is weakest: in SPX, the 2020 holdout OOS R^2 rises from -1.221 to -0.012 , and in RUT, the 2020 holdout rises from -0.587 to 0.294 .

The summary statistics point in the same direction. Pooled OOS R^2 rises from 0.221 to 0.364 in SPX and from 0.171 to 0.309 in RUT, and the mean OOS R^2 , mean RMSE, and mean correlation all improve consistently in both markets (Tables 5.4 and 5.5). These improvements are preserved when HAC-based inference is applied, so the out-of-sample gains are likewise not an artifact of a particular treatment of serial dependence. The improvement is, of course, not uniform across all holdout years: 2016 and 2018 in SPX, and 2018, 2022, and 2025 in RUT, show modest declines relative to the baseline. On the whole, however, the effect of the 3ETF specification cannot be attributed to a particular year.

Table 5.4: Year-by-year LOYO out-of-sample performance: SPX

Holdout year	Baseline			3ETF		
	R^2	RMSE (bp)	Corr.	R^2	RMSE (bp)	Corr.
2016	0.185	8.970	0.194	0.083	9.517	0.343
2017	0.074	10.069	0.226	0.246	9.083	0.426
2018	0.221	26.304	0.259	0.188	26.846	0.167
2019	0.023	8.934	-0.011	0.085	8.647	0.308
2020	-1.221	18.423	-0.294	-0.012	12.437	0.443
2021	0.416	7.600	0.064	0.695	5.494	0.079
2022	0.357	16.040	0.347	0.466	14.615	0.265
2023	0.571	15.725	0.438	0.683	13.509	0.505
2024	-0.016	15.428	0.589	0.188	13.792	0.701
2025	-0.022	11.980	0.242	0.094	11.276	0.474
Mean	0.059	13.947	0.205	0.272	12.522	0.371
Median	0.130			0.188		
Pooled	0.221			0.364		

Table 5.5: Year-by-year LOYO out-of-sample performance: RUT

Holdout year	Baseline			3ETF		
	R^2	RMSE (bp)	Corr.	R^2	RMSE (bp)	Corr.
2016	-0.350	12.787	0.069	0.155	10.120	0.260
2017	-0.152	10.498	0.142	0.010	9.734	0.341
2018	0.213	18.830	0.121	0.126	19.849	0.208
2019	-0.041	11.088	-0.007	-0.001	10.873	0.414
2020	-0.587	22.437	0.102	0.294	14.958	0.433
2021	0.477	12.368	0.431	0.517	11.895	0.375
2022	0.308	16.619	0.368	0.255	17.246	0.215
2023	0.661	13.922	0.354	0.757	11.782	0.454
2024	0.153	14.005	0.598	0.246	13.215	0.477
2025	0.064	18.193	0.248	-0.060	19.361	0.316
Mean	0.075	15.075	0.243	0.230	13.903	0.349
Median	0.108			0.200		
Pooled	0.171			0.309		

6 Robustness

6.1 Broad-Dollar Control: FX-Neutralization Robustness

To assess whether the explanatory power of the foreign-asset-based GBM terms merely reflects common variation in the U.S. dollar in disguise, this subsection conducts a robustness analysis using the broad-dollar index DTWEXBGS. Specifically, I divide the price indices of IEFA, IGOV, and IAU by the broad-dollar index to construct FX-neutralized series and recompute each asset’s log OLS slope from those series. Because DTWEXBGS does not align perfectly with the trading-day calendar of the asset price data, missing values are filled forward with the most recent observation.

6.1.1 In-Sample Performance

Table 6.1: In-sample performance: baseline versus FX-neutralized 3ETF extended specification

Market	R^2 (baseline)	R^2 (FXN 3ETF)	ΔR^2	$\Delta RMSE$ (bp)	ΔMAE (bp)
SPX	0.312	0.404	0.091	-0.906	-0.934
RUT	0.281	0.369	0.089	-0.887	-0.759

The explanatory gain of the 3ETF specification remains clearly intact after broad-dollar control (Table 6.1), with $\Delta R^2 = 0.091$ in SPX and $\Delta R^2 = 0.089$ in RUT—roughly on par with the original 3ETF specification (0.093 in SPX, 0.082 in RUT). In RUT, ΔR^2 even widens slightly after FX neutralization. The explanatory power of the foreign-asset components therefore does not reduce to a single broad-dollar common factor.

6.1.2 In-Sample Performance by Maturity Bin

Table 6.2: In-sample performance by τ bin: baseline versus FX-neutralized 3ETF extended specification

Market	Maturity bin	R^2 (baseline)	R^2 (FXN 3ETF)	ΔR^2	$\Delta RMSE$ (bp)	ΔMAE (bp)
SPX	1–2m	0.096	0.149	0.052	-0.666	-0.663
SPX	2–3m	0.184	0.270	0.086	-0.963	-0.767
SPX	3–5m	0.283	0.417	0.134	-1.338	-0.978
SPX	5–7m	0.373	0.548	0.174	-1.724	-1.097
SPX	7–10m	0.472	0.645	0.172	-1.756	-1.130
SPX	10–14m	0.525	0.618	0.093	-0.857	-0.879
SPX	14–21m	0.306	0.311	0.005	-0.048	-0.886
SPX	21m+	0.182	0.122	-0.059	0.483	-0.724
RUT	1–2m	0.112	0.164	0.051	-0.657	-0.547
RUT	2–3m	0.205	0.307	0.102	-1.038	-0.674
RUT	3–5m	0.254	0.375	0.120	-1.092	-0.822
RUT	5–7m	0.231	0.440	0.209	-1.843	-1.354
RUT	7–10m	0.284	0.475	0.192	-1.708	-1.106
RUT	10–14m	0.472	0.573	0.101	-1.060	-1.015
RUT	14–21m	0.482	0.526	0.044	-0.437	-0.484
RUT	21m+	0.413	0.283	-0.130	1.126	0.430

The maturity-bin pattern is largely preserved relative to the original 3ETF specification (Table 6.2). In both markets the gains concentrate in the medium-maturity range, with ΔR^2 peaking around 5–10 months, and turn negative in the 21-month-plus bin. The FX-neutralized 3ETF specification thus captures the medium-maturity low-frequency structure effectively but does not consistently improve the very long end. In RUT’s medium-maturity bins, ΔR^2 even widens slightly after FX neutralization, indicating that the foreign-asset components carry information beyond a simple dollar common factor.

6.1.3 Coefficient Structure

Table 6.3: In-sample regression coefficients: baseline versus FX-neutralized 3ETF extended specification

Regressor	SPX baseline	SPX + FXN 3ETF	RUT baseline	RUT + FXN 3ETF
Intercept	23.134*** (5.713)	18.586*** (4.394)	24.577*** (5.407)	15.815*** (3.822)
$GBM^{OIS,1Y}$	-0.548*** (0.170)	-0.0739 (0.124)	-0.555*** (0.124)	-0.188** (0.0730)
$GBM^{OIS,10Y}$	0.411** (0.172)	-0.111 (0.142)	0.541*** (0.130)	0.0926 (0.0898)
$GBM^{IEFA,FXN,70}$	—	-0.00778*** (0.00136)	—	-0.00605*** (0.000974)
$GBM^{IGOV,FXN,400}$	—	0.0178 (0.0127)	—	0.00113 (0.00989)
$GBM^{IAU,FXN,336}$	—	0.0208*** (0.00741)	—	0.0250*** (0.00498)
BAm^{ed}/τ	0.256*** (0.0635)	0.215*** (0.0653)	0.130*** (0.0225)	0.130*** (0.0262)
$NFCI$	-25.839** (10.359)	-37.721*** (8.005)	-23.961** (10.013)	-43.741*** (6.962)
R^2	0.3124	0.4036	0.2809	0.3695
Adj. R^2	0.3123	0.4034	0.2807	0.3692
RMSE (bp)	13.199	12.292	13.951	13.064
MAE (bp)	8.682	7.748	10.103	9.345

Notes: Standard errors in parentheses are date-based HAC (Newey–West) with maximum lag 21. ***, **, and * denote statistical significance at the 1%, 5%, and 10% levels, respectively.

Table 6.3 shows that the sign structure of the core asset components is largely preserved after broad-dollar control. The most robust findings concern the IEFA and IAU components: in both markets, $GBM^{IEFA,FXN,70}$ is negative and $GBM^{IAU,FXN,336}$ is positive, both significant at the 1% level even under lag 21 HAC standard errors. The $GBM^{IGOV,FXN,400}$ component, by contrast, retains a positive point estimate in both SPX and RUT but loses statistical significance in both markets.

The absorption of the OIS-based GBM terms moves in the same direction as in the original specification. In SPX, both $GBM^{OIS,1Y}$ and $GBM^{OIS,10Y}$ become insignificant once the asset components are added; in RUT, only $GBM^{OIS,1Y}$ remains significant at the 5% level, while $GBM^{OIS,10Y}$ weakens. A substantial portion of the low-frequency variation originally

captured by the OIS-based terms is therefore absorbed by the FX-neutralized asset-return components, with the degree of absorption not fully identical across the two markets. Under the conservative lag 21 HAC inference, some of the baseline-significance levels are also revised downward— $GBM^{OIS,10Y}$ and $NFCI$ in the SPX baseline, and $NFCI$ in the RUT baseline, are reported at the 5% rather than the 1% level. Even so, IEFA, IAU, BA^{med}/τ , and $NFCI$ remain the most stable explanatory variables in the extended specification.

The simultaneous loss of significance for the IGOV component in both markets after broad-dollar control carries economic content. Much of the explanatory power that $GBM^{IGOV,400}$ had in the original 3ETF specification appears to be attributable to the exchange-rate component embedded in international government bond returns—particularly to the broad-dollar cycle. Once the broad-dollar component is stripped out, only the pure duration–credit component of foreign sovereign bonds remains, and its alignment with the carry gap is not as structurally stable as that of foreign equity or gold. The IGOV explanatory power is therefore better read as leaning substantially on a dollar-cycle-mediated common-factor channel than as contributing to a FX-orthogonal outside-option channel.

This asymmetry suggests that the P→Q alignment documented here is not a single, homogeneous channel. Foreign equity (IEFA) and gold (IAU) remain robustly aligned with the carry gap even after the broad-dollar component is removed, and so are best read as a FX-orthogonal outside-option channel distinct from dollar exposure. Foreign sovereign bonds (IGOV), in contrast, appear to operate through a separate route mediated by the dollar cycle rather than through this FX-orthogonal channel. The P→Q alignment captured by the 3ETF specification is thus best understood as a heterogeneous structure superposing a FX-orthogonal investment-opportunity channel and a dollar-cycle-mediated channel.

6.1.4 Out-of-Sample Performance

Table 6.4: LOYO out-of-sample performance: baseline versus FX-neutralized 3ETF extended specification, summary

Market	Specification	Mean R^2	Median R^2	Pooled R^2	Mean RMSE (bp)	Mean Corr.
SPX	Baseline	0.059	0.130	0.221	13.947	0.205
SPX	FXN 3ETF	0.254	0.192	0.352	12.695	0.386
RUT	Baseline	0.075	0.108	0.171	15.075	0.243
RUT	FXN 3ETF	0.243	0.218	0.309	13.877	0.366

The out-of-sample improvements also persist after FX neutralization (Table 6.4). Pooled OOS R^2 rises from 0.221 to 0.352 in SPX and from 0.171 to 0.309 in RUT, with mean R^2 ,

median R^2 , mean RMSE, and mean correlation all improving in both markets. Compared with the original 3ETF specification, the out-of-sample performance of the FX-neutralized specification remains broadly comparable. Year-by-year results are reported in Tables 6.5 and 6.6.

Table 6.5: Year-by-year LOYO out-of-sample performance: SPX, FX-neutralized 3ETF specification

Holdout year	Baseline			FXN 3ETF		
	R^2	RMSE (bp)	Corr.	R^2	RMSE (bp)	Corr.
2016	0.185	8.970	0.194	-0.144	10.629	0.376
2017	0.074	10.069	0.226	0.273	8.923	0.425
2018	0.221	26.304	0.259	0.167	27.196	0.193
2019	0.023	8.934	-0.011	0.194	8.114	0.401
2020	-1.221	18.423	-0.294	0.017	12.256	0.431
2021	0.416	7.600	0.064	0.511	6.955	0.096
2022	0.357	16.040	0.347	0.498	14.174	0.291
2023	0.571	15.725	0.438	0.649	14.213	0.504
2024	-0.016	15.428	0.589	0.185	13.820	0.686
2025	-0.022	11.980	0.242	0.189	10.671	0.458
Mean	0.059	13.947	0.205	0.254	12.695	0.386
Median	0.130			0.192		
Pooled	0.221			0.352		

Table 6.6: Year-by-year LOYO out-of-sample performance: RUT, FX-neutralized 3ETF specification

Holdout year	Baseline			FXN 3ETF		
	R^2	RMSE (bp)	Corr.	R^2	RMSE (bp)	Corr.
2016	-0.350	12.787	0.069	0.188	9.916	0.304
2017	-0.152	10.498	0.142	0.039	9.591	0.340
2018	0.213	18.830	0.121	0.118	19.941	0.222
2019	-0.041	11.088	-0.007	0.084	10.399	0.456
2020	-0.587	22.437	0.102	0.248	15.440	0.415
2021	0.477	12.368	0.431	0.492	12.198	0.408
2022	0.308	16.619	0.368	0.250	17.307	0.209
2023	0.661	13.922	0.354	0.737	12.269	0.452
2024	0.153	14.005	0.598	0.252	13.162	0.488
2025	0.064	18.193	0.248	0.027	18.548	0.367
Mean	0.075	15.075	0.243	0.243	13.877	0.366
Median	0.108			0.218		
Pooled	0.171			0.309		

The year-by-year results show that the improvement of the FX-neutralized 3ETF specification is not driven by any single year: 8 of 10 holdout years for SPX and 7 of 10 for RUT yield higher OOS R^2 than the baseline. The gains are most pronounced where the baseline was weakest—OOS R^2 rises from -1.221 to 0.017 in the 2020 SPX holdout, and from -0.587 to 0.248 in the 2020 RUT holdout. Some years show modest declines, however, so the advantage of the FX-neutralized specification is best read as an average improvement repeated across most years rather than a uniform gain in every year.

Taken together, the core explanatory power of the 3ETF specification is largely preserved after a coarse broad-dollar neutralization. The foreign-equity and gold outside-option components remain comparatively robust, both in their in-sample coefficients and in their out-of-sample performance. The international government bond component, by contrast, weakens in significance and in cross-market consistency, indicating greater exposure to currency factors. The FX-neutralized robustness analysis therefore shows that the foreign-asset-based explanatory power is not generated solely by a dollar common factor, while also showing that the most robust channels within it are foreign equity and gold.

6.2 Alternative Asset Combinations

To assess whether the main 3ETF specification depends on a particular asset combination, this subsection examines two alternative 3ETF specifications: a U.S.-centered combination

(VTI at 60 trading days, BND at 252, IAU at 300) and an emerging-market-centered combination (IEMG at 70, EBND at 210, IAU at 300). The lookback windows for each combination are selected through a separate horizon scan.

Table 6.7: Performance comparison across alternative 3ETF asset combinations

Specification	SPX IS R^2	RUT IS R^2	SPX mean OOS R^2	RUT mean OOS R^2	SPX pooled OOS R^2	RUT pooled OOS R^2
Baseline	0.312	0.281	0.059	0.075	0.221	0.171
Main 3ETF	0.405	0.363	0.272	0.230	0.364	0.309
US only	0.368	0.347	0.224	0.194	0.308	0.261
Emerging	0.387	0.359	0.247	0.256	0.332	0.341

Notes: Main 3ETF = IEFA(70) + IGOV(400) + IAU(336); US only = VTI(60) + BND(252) + IAU(300); Emerging = IEMG(70) + EBND(210) + IAU(300). The lookback window for each alternative specification is selected through a separate horizon scan. Out-of-sample performance reports the LOYO mean and pooled R^2 .

Table 6.7 compares the three alternative specifications side by side. Three patterns emerge.

First, all three alternatives improve in- and out-of-sample performance relative to the baseline, indicating that the alignment with the carry gap is not specific to a single asset combination.

Second, in SPX the developed ex-U.S. specification adopted in the main analysis delivers the strongest performance on both in-sample and out-of-sample metrics. In RUT, however, the emerging-market specification exceeds the main specification out of sample, suggesting that in the small-cap options market emerging-market components may carry comparatively richer outside-option information.

Third, both foreign-tilted specifications outperform the U.S.-only specification overall. This is consistent with the paper’s interpretation that the opportunity-cost channel linked to the carry gap is more sharply visible across a broader global investment- opportunity set than within U.S. domestic asset classes.

7 Discussion

This section consolidates the economic content of the empirical results and discusses both their interpretive scope and their limitations. The emphasis is not only on the explanatory gain itself but on which channels remain robust under HAC inference and FX neutralization, and how those patterns differ between SPX and RUT.

7.1 Empirical Implications of the P–Q Channel

The most direct implication of the analysis lies in the absorption pattern: a substantial portion of the low-frequency variation captured by the OIS terms in the baseline is taken over by the physical-measure asset-return components. This finding does not diminish the usefulness of the risk-neutral framework. It indicates, rather, that while the framework suffices for pricing the terminal payoff, it does not internalize the economic burden that arises along the pre-maturity enforcement path. The opportunity cost faced by the parity enforcer is not defined inside Q, and if that cost is a function of P-measure investment opportunities, then information transmission in the P→Q direction is unavoidable.

What is essential to this interpretation is that adding the 3ETF components is not simply a matter of inserting new regressors: structures previously captured by the baseline indirectly through the OIS—a Q-measure component—are taken over by P-measure asset returns more directly. The most striking example is the SPX $GBM^{OIS,10Y}$ coefficient, which flips from positive to negative, and more generally the sharp loss of significance of the OIS-based components under HAC inference.

This absorption is not complete or uniform, however. In SPX, both $GBM^{OIS,1Y}$ and $GBM^{OIS,10Y}$ become insignificant once the 3ETF components are included, and much of the prior OIS-based low-frequency structure is taken over by the asset-return components. In RUT, $GBM^{OIS,1Y}$ remains significant while only $GBM^{OIS,10Y}$ weakens or turns insignificant. The P→Q channel is therefore present in both markets, but it appears as a stronger displacement relation in SPX and as a partial-absorption structure in RUT, where the asset-return and short-horizon OIS components coexist.

7.2 Relative Strength of Foreign-Asset Explanatory Power

As Figure 4.1 shows, the pattern of foreign assets delivering relatively stronger explanatory power than U.S. domestic assets is already visible at the single-asset stage. In equities, IEFA and IEMG yield larger incremental R^2 than VTI; in bonds, IGOV exceeds BND and SCHP; and in real estate, VNQI exceeds VNQ.

This pattern is confirmed more systematically in the alternative- combination analysis of Section 6. Table 6.7 shows that the U.S.-only specification (VTI + BND + IAU) provides a meaningful improvement over the baseline but is systematically weaker than both the emerging-market specification (IEMG + EBND + IAU) and the developed ex-U.S. specification (IEFA + IGOV + IAU) adopted in the main analysis, in- and out-of-sample. The outside-option information aligned with the carry gap is therefore not confined to U.S. assets, but is more sharply visible in the global investment-opportunity set than within U.S.

domestic asset classes.

It would be an overreading, however, to conclude that “any foreign asset is strong.” Under HAC-based inference, robustness varies clearly across foreign assets as well. IEFA and IAU retain stable sign and significance across both markets, whereas IGOV is strong in SPX but weak or insignificant in RUT, a pattern broadly preserved under the broad-dollar-neutralized FX-neutralized specification. The core of the foreign-asset story is not that all foreign assets are uniformly strong, but that foreign equity and gold reappear as particularly robust outside-option components.

The precise mechanism behind this relative strength lies beyond the scope of this paper. Possibilities include foreign assets providing opportunity-cost signals more independent of components internal to the U.S. options market, and the outside-option structure of global asset allocation reflecting more directly the realistic alternatives of the parity enforcer than U.S. internal capital opportunity costs. The greater cross-market instability of the IGOV channel further suggests that the explanatory power of the foreign-bond component is intertwined not only with a pure outside-option effect but also with currency factors and market-specific microstructure.

7.3 Common Structure and Cross-Market Heterogeneity

SPX and RUT share a common carry-gap structure but differ distinctly in the sensitivity of certain explanatory channels. In both markets, the IEFA component is the most robust in terms of sign and significance, with out-of-sample improvements in many holdout years. This suggests that the two markets share a common risk-bearing-capacity channel reflected in the low-frequency variation of global risk assets.

In greater detail, however, distinct cross-market heterogeneity overlays the common structure. First, the degree of OIS-component absorption differs. In SPX, all OIS-based GBM terms become insignificant under HAC inference once the asset-return components are added, whereas in RUT $GBM^{OIS,1Y}$ remains significant at the 5% level. Second, the proxy for the safe-asset channel splits across markets. In SPX, the IGOV coefficient is significant at the 1% level even at lag 21, while the IAU point estimate is positive but does not reach conventional significance. RUT shows the reverse: IAU is robustly significant at the 1% level, while IGOV preserves its sign but lacks significance. Third, the alternative-combination analysis finds that the emerging-market specification exceeds the main specification out of sample in RUT, suggesting that RUT may respond to a broader range of safe-asset proxies than SPX.

The cross-market asymmetry between IGOV and IAU may be linked to differences in the risk-off dimension that the two proxies capture. The low-frequency component of IGOV is

not a purely asset-specific channel but partially shares the character of a rate-like object, and it may therefore behave as a variable that splits explanatory power with the OIS-based terms of the baseline regression. The weakening of the IGOV coefficient in RUT under HAC inference and under the FX-neutralized specification is consistent with this reading. IAU, by contrast, can be read as a more nearly pure safe-haven-demand proxy with less overlap with rate-like components. SPX, as a large-cap index, is more directly exposed to global interest-rate factors, so a rate-like safe-asset proxy such as IGOV may better capture variation in the enforcer’s capacity. RUT, as a small-cap index, may be more sensitive to pure safe-haven-demand phases—the dimension captured by IAU—than to global interest rates. Under this reading, the cross-market asymmetry between the two proxies reflects not the absence of a safe-asset channel but differences in the risk-off dimension to which each market is more sensitive.

The two markets are therefore best understood not as symmetrically exposed to an identical implementation-risk-premium structure but as sharing a common risk-bearing-capacity channel (IEFA) while differing in the proxy through which the safe-asset dimension appears. SPX further shows the asset-return components more directly displacing the prior OIS-based low-frequency structure, whereas RUT exhibits a mixed structure in which the asset-return and short-horizon OIS components coexist. P-measure capacity components absorb the prior Q-measure-internal components more aggressively in SPX, while the two channels coexist to a greater extent in RUT. This difference suggests that the underlying-asset character and the composition of the enforcers exposed to each market may not be fully identical, but a structural identification of those differences lies beyond the scope of this paper and is left for future research.

7.4 Asset-Pricing Interpretation

The observed P→Q alignment structure also carries implications that admit an asset-pricing interpretation. The paper does not directly test a particular asset-pricing model, but the observed structure has several points of contact with established theoretical frameworks.

First, the loading of multiple asset classes on the carry gap at distinct horizons is conceptually consistent with the ICAPM of [Merton \(1973\)](#), in which investors hedging variation in the future investment-opportunity set are exposed to multiple state variables with heterogeneous time structures. The finding that IEFA, IGOV, and IAU deliver explanatory power at horizons of 70, 400, and 336 trading days, respectively, suggests that the opportunity cost of parity enforcement does not reduce to a single representative asset or single time scale and may instead be composed of multiple low-frequency state variables.

Second, the asset-class sign structure is consistent with a story in which the capital commitment of parity enforcement operates asymmetrically across risk-on/risk-off regimes. The negative coefficient on IEFA, a risk asset, suggests that the incentive to tie up capital in parity enforcement weakens when the expected opportunity in external risk assets is favorable. The positive coefficient on IAU, and the—particularly in SPX stronger—positive coefficient on IGOV, are consistent with a safe-asset-demand or risk-off channel. This sign structure, too, does not hold uniformly across all asset classes. The HAC and FX-neutralized results together identify IEFA and IAU as the most robustly recurring components, while IGOV emerges as a more conditional, market- dependent channel. An honest asset-pricing reading therefore views the three asset classes not as a fully symmetric multi-factor structure, but as a robust core channel anchored by foreign equity and gold, with foreign government bonds layered on more selectively.

The fact that this sign structure remains robust for IEFA and IAU even after broad-dollar FX neutralization (Table 6.3) supports the view that the observed alignment reflects a more fundamental opportunity-cost channel rather than an indirect representation of a dollar common factor. The weakening of IGOV, by contrast, leaves open the possibility that the foreign-bond return component is a composite combining currency, interest-rate, and market-structure factors rather than a direct outside-option channel.

These interpretations cannot be settled by the present reduced-form results alone. Identifying whether the observed alignment plays the role of an ICAPM state variable or reflects a different structural mechanism requires more structural model specification and testing, and is left for future research.

7.5 Extension Beyond Put–Call Parity

The interpretation developed here need not be confined to put–call parity in equity index options. More generally, any arbitrage involving a futures or forward leg and exposed to interim mark-to-market losses, variation margin, and finite-capital constraints may admit a similar implementation-risk term in systematic operation. On this view the GBM term is best read not as a reduced-form artifact specific to a particular options-market regime, but as a reduced-form object summarizing the broader parity-enforcement environment that converts a terminal no-arbitrage relation into a path-dependent capital-using strategy.

Preliminary evidence is consistent with this interpretation. In a post-GFC sample, an exploratory regression of the government-bond CIP deviation residual on a fixed three-asset specification scaled by the trailing 42-trading-day FX volatility yields an R^2 of roughly 0.64. These results remain preliminary, and the measurement target and market structure

differ from the main analysis, so they cannot be read as a structural validation of the same mechanism. They do, however, suggest that the $P \rightarrow Q$ alignment documented here is unlikely to be a phenomenon specific to equity index options, and may reproduce in the broader class of parity relations involving futures or forward intermediation. A systematic analysis of this is left for separate future work.

7.6 Limitations and Future Research

This paper is a reduced-form empirical analysis and therefore does not fully establish the causal pathway underlying the observed alignment. Assessing the generality of the results also requires additional validation across different underlying assets, options markets, and functional forms.

A particularly important limitation is that the observed alignment does not repeat uniformly across all asset classes and markets. IEFA and IAU are comparatively robust, but IGOV weakens in some markets, and the absorption of the OIS-based components also differs between SPX and RUT. Rather than weakening the central result, this suggests that the opportunity-cost structure of parity enforcement may not reduce to a single representative channel. The task for future research is therefore to move beyond “does the alignment exist?” to a structural account of “which assets operate more strongly in which markets, and why?”

Three more concrete directions follow. First, explaining why foreign equity and gold remain robust while foreign government bonds are less stable will require additional analyses that decompose currency exposure, duration, safe-asset demand, and global interest-rate regimes. Second, the interpretation here need not be confined to equity index options: similar implementation-risk and capital-commitment channels may operate in other derivatives markets in which parity relations exist—FX, commodities, fixed income—and the connection to CIP deviations is a particularly interesting candidate. Third, identifying whether the observed horizon heterogeneity reflects an ICAPM-style state-variable structure will require more structural model testing.

8 Conclusion

This paper has shown that physical-measure asset returns load systematically on the put-call-parity-based carry gap, a Q -measure object. Under the standard risk-neutral framework, P -measure asset returns have no structural reason to load on this object. Nevertheless, augmenting the baseline specification with the low-frequency return components of IEFA,

IGOV, and IAU raises the explanatory power of the carry gap by $\Delta R^2 = 0.093$ in SPX and $\Delta R^2 = 0.082$ in RUT, and lifts pooled out-of-sample R^2 from 0.221 to 0.364 in SPX and from 0.171 to 0.309 in RUT. These gains survive broad-dollar FX neutralization, and alternative combinations built from U.S. or emerging-market assets also improve on the baseline but remain weaker than the developed ex-U.S. specification adopted in the main analysis.

The results contribute to the literature in three ways.

First, the paper provides systematic empirical evidence of a P→Q channel through which P-measure investment opportunities shape the enforcement burden of Q-measure pricing relations. Whereas the existing literature has focused on the Q→P direction—recovering P-measure expected returns from Q-measure objects—this paper shows that the reverse channel exists and operates through the opportunity-cost structure of parity enforcement. The sharpest evidence is the absorption pattern: after the 3ETF components are introduced, much of the low-frequency variation previously captured by the OIS-based GBM terms is taken over by physical-measure returns.

Second, the effective horizon at which each asset class aligns with the carry gap differs sharply across assets (IEFA: 70 trading days; IGOV: 400; IAU: 336). This horizon heterogeneity suggests that the opportunity-cost structure of parity enforcement does not reduce to a single representative asset or common frequency but is composed of multiple low-frequency components.

Third, the asset classes with the strongest explanatory power are repeatedly concentrated in non-U.S. markets, and a specification built solely from U.S. assets is systematically weaker than the non-U.S.-centered specifications, both in- and out-of-sample. The outside-option channel for parity enforcement is therefore linked to a global investment-opportunity set broader than U.S. domestic asset classes.

This paper is a reduced-form empirical analysis and does not directly identify the structural mechanism behind the observed P→Q alignment. Determining whether the heterogeneous horizon loadings of the multiple asset classes reflect an ICAPM state-variable structure or operate through a different route requires more structural model specification and testing, which is left for future research. Nevertheless, by documenting that the residual of the most model-free no-arbitrage relation is not separable from physical-measure investment opportunities, the paper shows that risk-neutral pricing is structurally silent on the economic burden of the enforcement process.

Funding

This research did not receive any specific grant from funding agencies in the public, commercial, or not-for-profit sectors.

Declaration of AI usage in manuscript preparation

During the preparation of this manuscript, the author used ChatGPT (OpenAI) and Claude (Anthropic) for language refinement and structural clarity. All outputs were reviewed and edited by the author, who takes full responsibility for the content.

Declaration of interest

The author declares no competing interests.

References

- Stoll, H. R. (1969). The Relationship between Put and Call Option Prices. *The Journal of Finance*, 24(5), 801–824. <https://doi.org/10.1111/j.1540-6261.1969.tb01694.x>
- Merton, R. C. (1973). An Intertemporal Capital Asset Pricing Model. *Econometrica*, 41(5), 867–887. <https://doi.org/10.2307/1913811>
- Gould, J. P., & Galai, D. (1974). Transaction Costs and the Relationship between Put and Call Prices. *Journal of Financial Economics*, 1(2), 105–129. [https://doi.org/10.1016/0304-405X\(74\)90001-4](https://doi.org/10.1016/0304-405X(74)90001-4)
- Klemkosky, R. C., & Resnick, B. G. (1979). Put–Call Parity and Market Efficiency. *The Journal of Finance*, 34(5), 1141–1155. <https://doi.org/10.1111/j.1540-6261.1979.tb00061.x>
- Shleifer, A., & Vishny, R. W. (1997). The Limits of Arbitrage. *The Journal of Finance*, 52(1), 35–55. <https://doi.org/10.1111/j.1540-6261.1997.tb03807.x>
- Ackert, L. F., & Tian, Y. S. (2001). Efficiency in Index Options Markets and Trading in Stock Baskets. *Journal of Banking & Finance*, 25(9), 1607–1634. [https://doi.org/10.1016/S0378-4266\(00\)00145-X](https://doi.org/10.1016/S0378-4266(00)00145-X)
- Gromb, D., & Vayanos, D. (2002). Equilibrium and Welfare in Markets with Financially Constrained Arbitrageurs. *Journal of Financial Economics*, 66(2–3), 361–407. [https://doi.org/10.1016/S0304-405X\(02\)00228-3](https://doi.org/10.1016/S0304-405X(02)00228-3)
- Ofek, E., Richardson, M., & Whitelaw, R. F. (2004). Limited arbitrage and short sales restrictions: evidence from the options markets. *Journal of Financial Economics*, 74(2), 305–342. <https://doi.org/10.1016/j.jfineco.2003.05.008>
- Bollerslev, T., Tauchen, G., & Zhou, H. (2009). Expected Stock Returns and Variance Risk Premia. *The Review of Financial Studies*, 22(11), 4463–4492. <https://doi.org/10.1093/rfs/hhp008>
- Brunnermeier, M. K., & Pedersen, L. H. (2009). Market Liquidity and Funding Liquidity. *The Review of Financial Studies*, 22(6), 2201–2238. <https://doi.org/10.1093/rfs/hhn098>
- Mitchell, M., & Pulvino, T. (2012). Arbitrage Crashes and the Speed of Capital. *Journal of Financial Economics*, 104(3), 469–490. <https://doi.org/10.1016/j.jfineco.2011.09.002>

- Ross, S. (2015). The Recovery Theorem. *The Journal of Finance*, 70(2), 615–648. <https://doi.org/10.1111/jofi.12092>
- Martin, I. (2017). What Is the Expected Return on the Market? *The Quarterly Journal of Economics*, 132(1), 367–433. <https://doi.org/10.1093/qje/qjw034>
- Du, W., Tepper, A., & Verdelhan, A. (2018). Deviations from Covered Interest Rate Parity. *The Journal of Finance*, 73(3), 915–957. <https://doi.org/10.1111/jofi.12620>
- Azzone, M., & Baviera, R. (2021). Synthetic Forwards and Cost of Funding in the Equity Derivative Market. *Finance Research Letters*, 41, 101841. <https://doi.org/10.1016/j.frl.2020.101841>
- Muravyev, D., Pearson, N. D., & Pollet, J. M. (2025). Why does options market information predict stock returns? *Journal of Financial Economics*, 172, 104153. <https://doi.org/10.1016/j.jfineco.2025.104153>
- Shin, U. (2026). The Cost of a Free Lunch. *SSRN Working Paper*, No. 6407379 https://papers.ssrn.com/abstract_id=6407379
- Board of Governors of the Federal Reserve System (US) (2026a). Federal Reserve Bank of Chicago, Chicago Fed National Financial Conditions Index [NFCI], retrieved from FRED, Federal Reserve Bank of St. Louis, April 3, 2026. <https://fred.stlouisfed.org/series/NFCI>.
- Board of Governors of the Federal Reserve System (US) (2026b). Board of Governors of the Federal Reserve System (US), Nominal Broad U.S. Dollar Index [DTWEXBGS], retrieved from FRED, Federal Reserve Bank of St. Louis, April 3, 2026. <https://fred.stlouisfed.org/series/DTWEXBGS>.

A Data and Methodological Details

This appendix collects the implementation details of the data, identification procedure, variable construction, sample cleaning, and regression evaluation used in the main text. The body of the paper focuses on the core intuition and main results; this appendix supplements that with the concrete procedures needed for replication.

A.1 Data and Analysis Sample

I identify market-implied discounting factors from SPX and RUT options and construct the carry gap by comparing them with the OIS discounting factor. The implied discount factors are identified using the synthetic-forward procedure of [Azzone and Baviera \(2021\)](#), the central advantage of which is that the discount factor implicitly applied by the market can be recovered from European call and put prices alone at a common maturity.

Option quote data are minute-level NBBO from ThetaData. The option data extend through December 31, 2025, but the analysis sample is restricted to January 4, 2016 through October 31, 2025 to match the availability of the OIS data. All results in the body of the paper are based on the common sample on which both the option-market information and the OIS discount curve are simultaneously observable.

SPX and RUT options are European-style index options, so they carry no early-exercise premium, which removes a source of institutional noise from parity-based discount-factor identification.

The empirical analysis is implemented in MATLAB R2025b.²

²In a parallel computing environment, the full pipeline ran in roughly one hour for the two markets combined.

A.2 Identification of Option-Implied Discount Factors

The basic identification logic follows [Azzone and Baviera \(2021\)](#). For European calls and puts at time t sharing maturity T and strike K , put–call parity is

$$C_t(K, T) - P_t(K, T) = B_t(T)(F_t(T) - K), \quad (8)$$

where $B_t(T)$ is the market-implied discounting factor and $F_t(T)$ the forward value at the same maturity.

Defining the synthetic forward as

$$\mathcal{G}_t(K, T) = C_t(K, T) - P_t(K, T), \quad (9)$$

no-arbitrage requires the forward value to be independent of K , so the market-implied discounting factor is identified as the value that makes

$$F_t(T) = \frac{\mathcal{G}_t(K, T)}{B_t(T)} + K \quad (10)$$

flat across strikes.

In implementation, for each date–maturity combination I jointly estimate $\hat{B}_t(T)$ and $\hat{F}_t(T)$ from the linear relation between the synthetic forward and strike across the cross-section of strikes. The option-implied discount factor is therefore the discounting coefficient that makes the forward price recovered from the synthetic forward flat across strikes.

This procedure reduces dependence on a particular ATM contract or any chosen money-

ness range, removes the need to treat dividend estimates as a separate exogenous input, and mitigates the non-synchronicity problems that arise when spot, futures, interest-rate, and dividend data must be combined separately.

A.3 OIS Curve Construction and Carry-Gap Computation

The benchmark is the OIS discounting factor. Since the global financial crisis, the OIS curve has become the standard discounting benchmark for derivatives, and [Azzone and Baviera \(2021\)](#) likewise measure the funding spread against it.

I apply standard bootstrapping to daily OIS data to recover discounting factors and zero rates by maturity, then construct maturity-matched OIS discounting factors aligned with the option maturities and compare them directly to $\hat{B}_t(T)$.

The carry gap is the annualized wedge between the two. Letting $\tau_t(T) = T - t$,

$$CG_t(T) = \frac{1}{\tau_t(T)} \log \left(\frac{D_t^{\text{OIS}}(T)}{\hat{B}_t(T)} \right), \quad (11)$$

where $D_t^{\text{OIS}}(T)$ is the OIS-based discounting factor and $\hat{B}_t(T)$ the option-implied discounting factor. $CG_t(T) > 0$ indicates that the options market embeds a higher implied carry than the OIS benchmark.

In the empirical analysis I use the basis-points version

$$CG_t^{bp}(T) = 10^4 \cdot CG_t(T), \quad (12)$$

and the daily-aggregated market-level carry gap is denoted $CG_{i,t}^{bp}$.

A.4 Sample Cleaning and Daily Aggregation

The purpose of preprocessing is to drop observations with very low liquidity or unstable price information so that the cross-sectional regression remains stable. I retain only call–put pairs that share the same strike and maturity, and exclude observations with abnormally low prices or excessive bid–ask spreads. I also exclude maturities with too few effective strikes for stable cross-sectional identification, and dates on which OIS curve construction fails or the term structure is anomalous.

The final sample consists of observations for which (i) the option- implied discounting factor is identifiable and (ii) the OIS discounting factor can be stably constructed at the same date and maturity. For each of SPX and RUT, I build a date \times maturity panel and aggregate to the daily series using the median of the eligible observations on each date. This approach reduces sensitivity to outliers and transitory noise while still tracking the central movement of the carry gap.

A.5 Construction of the Asset-Return-Based Low-Frequency Component

The asset-return extension in the main text uses ETF price data representing the major asset classes to construct the low-frequency return component. The ETFs are VTI, IEFA, IEMG, BND, SCHP, IGOV, EBND, IAU, VNQ, and VNQI, chosen to represent U.S. equity, developed ex-U.S. equity, emerging-market equity, U.S. aggregate bond, U.S. inflation-linked bond, international government bond, emerging-market sovereign bond, gold, U.S. REITs, and ex-U.S. REITs, respectively.

For each ETF, I estimate the low-frequency component by OLS on the log-price path over the most recent n trading days through $t - 1$. The n -day low-frequency return component for asset a is the slope $\beta_{a,t}^{(n)}$ from

$$\log P_{a,t-1-j} = \alpha_{a,t}^{(n)} + \beta_{a,t}^{(n)} j + u_{a,t-1-j}, \quad j = 0, 1, \dots, n - 1. \quad (13)$$

For brevity I refer to this as the log OLS slope. Computing it from information through $t - 1$ only, excluding the contemporaneous price at date t , precludes look-ahead bias.

I use the log OLS slope rather than a simple cumulative return because it reflects persistent trend components more stably than transient spikes. This component then serves as the rate-like object of the asset-return-based GBM term.

A.6 Regression Estimation and Performance Evaluation

The baseline and 3ETF extended specifications are both estimated as separate regressions for SPX and RUT. The baseline includes the OIS-based GBM terms, the bid–ask term, and NFCI; the extended specification adds the asset-return-based GBM terms for IEFA, IGOV, and IAU.

Inference on the regression coefficients uses date-based HAC (Newey–West) standard errors, which jointly mitigate heteroskedasticity and possible low-order autocorrelation in the residuals of a daily time-series regression. Unless otherwise noted, all parenthesized standard errors and significance markers in the coefficient tables of the main text and appendix are based on these HAC standard errors. In the implementation, the maximum lag length is set to 21.

Out-of-sample evaluation uses leave-one-year-out (LOYO) validation. For each year, I exclude that year as the holdout sample, estimate the regression coefficients on the remaining years, and compute fit and prediction errors on the excluded year.

The performance metrics are in-sample R^2 , adjusted R^2 , RMSE, and MAE, together with year-by-year out-of-sample R^2 , mean R^2 , median R^2 , pooled R^2 , mean RMSE, and mean correlation under the LOYO scheme. The in-sample and out-of-sample fit metrics themselves summarize point-estimate performance; the HAC adjustment applies primarily to standard errors and significance assessment. All OOS results reported in the main text and appendix are based on this procedure.